Development of two novel benzoylphenylurea sulfur analogues and evidence that the microtubule-associated protein *tau* is predictive of their activity in pancreatic cancer

Antonio Jimeno,[1] Gurulingappa Hallur,[2] Audrey Chan,[1] Xiangfeng Zhang,[1] George Cusatis,[1] Fonda Chan,[1] Preeti Shah,[1] Rongbing Chen,[1] Ernest Hamel,[4] Elizabeth Garrett-Mayer,[3] Saeed Khan,[2] and Manuel Hidalgo[1]

[1]Gastrointestinal Cancer Program, [2]Chemical Therapeutics Program, and [3]Division of Statistics, Sidney Kimmel Comprehensive Cancer Center, The Johns Hopkins University School of Medicine and [4]Toxicology and Pharmacology Branch, Developmental Therapeutics Program, Division of Cancer Treatment and Diagnosis, National Cancer Institute at Frederick, NIH

Abstract

In this work, we evaluated two lead compounds, referred to as SG410 and SG430, obtained from a screen of sulfur benzoylphenylurea analogues, against *in vitro* and *in vivo* models of pancreas cancer. Both drugs showed a similar mechanism of action profile, with SG410 being more potent as an inhibitor of tubulin assembly. We determined the best *in vivo* administration schedule and tested SG410 and SG430 in nine cases of a novel platform of direct pancreas cancer xenografts. Both compounds had antiproliferative activity *in vitro* in the low nanomolar range, but only SG410 showed significant activity *in vivo*. Administration of SG410 resulted in significant tumor growth delay in five of nine groups tested. In a direct comparison in three of the cases, SG410 was at least as efficacious as docetaxel. We also sought markers that would be predictive of the efficacy of these agents, and we found such a marker in microtubule-associated protein *tau* (MAPT). This protein enhances the assembly and stability of microtubules. In both the cell lines and the direct human xenografts, MAPT mRNA and protein levels correlated well. There was also a statistically significant inverse correlation between MAPT expression and sensitivity to the tested agents. In summary, the novel sulfur benzoylphenylurea SG410 showed activity inversely related to MAPT expression in a preclinical model of pancreatic cancer comparable with that observed with docetaxel, another microtubule-targeting agent. [Mol Cancer Ther 2007;6(5):1509–16]

Introduction

Pancreatic cancer is a devastating disease, with the incidence and mortality rates almost identical (1). At the time of diagnosis, 80% of patients have locally advanced or metastatic disease for which no curative therapy exists. Moreover, 80% of patients treated with curative intent will have recurrent disease within 2 years of surgical resection and will succumb to their disease (2). Only two agents are formally approved for this patient population: gemcitabine and erlotinib. Although microtubules play an important role in a variety of cellular process, including mitosis and cell division (3, 4), thus far, these compounds play no role in the treatment of pancreatic cancer. Clinically useful antitubulin agents fall into two major classes: (*a*) microtubule stabilizers, such as paclitaxel and docetaxel, which prevent the depolymerization of tubulin (5); and (*b*) *Catharanthus* (formerly *Vinca*) alkaloids (vincristine, vinblastine, and vinorelbine), which inhibit the polymerization of tubulin and numerous other classes of compounds that interact with tubulin, including a large group that inhibit the binding of colchicine to tubulin and are therefore referred to as colchicine site agents (5).

Benzoylphenylureas were initially developed as insecticides but, during random screening, were found to possess *in vitro* and *in vivo* antitumor activity (6). To improve physicochemical properties, a number of analogues were synthesized, including water-soluble derivatives (7, 8). Six of these compounds were screened at the National Cancer Institute for their cytotoxicity against various cancer cell lines. They exhibited potent antitumor activity *in vitro* against several cancer cell lines as well as *in vivo* against several tumor models. The lead compound from that initial screening, *N,N*-dimethylamino-benzoylphenylurea (NSC 639829), is under clinical development (9, 9a). To further improve the potency of this class of compounds, additional analogues are being synthesized and tested (10). A family of sulfur-containing derivatives was found to be particularly effective against prostate, breast and pancreas cancer cell lines (11). Two of these compounds (SG410 and SG430) were selected for further characterization and testing against a broader panel of pancreas cancer cell lines. Their superior *in vitro* activity led us to examine their effects as

Received 9/25/06; revised 2/26/07; accepted 3/29/07.

The costs of publication of this article were defrayed in part by the payment of page charges. This article must therefore be hereby marked *advertisement* in accordance with 18 U.S.C. Section 1734 solely to indicate this fact.

Note: S. Khan and M. Hidalgo contributed equally to this work.

Requests for reprints: Manuel Hidalgo, Room 1M88, 1650 Orleans Street, Baltimore, MD 21231-1000. Phone: 410-502-3850; Fax: 410-614-9006. E-mail: mhidalg1@jhmi.edu and Saeed Khan, Room 1M51, 1650 Orleans Street, Baltimore, MD 21231-1000. Phone: 410-614-0200; Fax: 410-614-8397. E-mail: khansa@jhmi.edu

doi:10.1158/1535-7163.MCT-06-0592

well in *in vivo* models. For *in vivo* evaluation, we used a new platform consisting of xenografts developed by implanting directly tumor material from pancreatic cancer surgical specimens in nude mice (12). Histologic and molecular studies show that these tumors (*a*) maintain the genetic features of the original cancer, (*b*) represent the heterogeneity of pancreatic cancer well, and (*c*) do not change over time.

Although there are many new agents entering clinical development, often, there is no information on biomarkers that may predict the activity of these drugs. Consequently, there is very little data to prioritize which agents should be administered to a given patient. One of the objectives of our work was to define biomarkers predicting the efficacy of the benzoylphenylurea derivatives. The microtubule-associated protein *tau* (MAPT) is a microtubule-binding protein believed to be important for the assembly and stabilization of microtubules. In normal adult human brain, there are six isoforms of MAPT, produced from a single gene by alternative mRNA splicing (13–15). MAPT was shown to be related to microtubule stability, and its level of expression has been negatively correlated with sensitivity to both paclitaxel and docetaxel, two anticancer agents targeting the microtubule system (16, 17). Another marker that has been correlated with the activity of anti-microtubule agents is tubulin. Seve et al. reported that class III β-tubulin expression level is predictive of response to paclitaxel in non–small-cell lung cancer (18), and somatic mutation of class I β-tubulin have been linked to paclitaxel resistance (19).

In this work, we aimed at characterizing the *in vitro* and *in vivo* efficacy of SG410 and SG430, focusing in pancreatic cancer, and determining whether tumor levels of related markers, such as MAPT or class III β-tubulin, would predict the efficacy of these agents.

Materials and Methods

Drugs

SG410 and SG430 were synthesized as previously described (ref. 11; structures in Fig. 1A). For *in vitro* analysis, the drugs were dissolved in DMSO, and for *in vivo* studies, the drugs were dissolved in 5% DMA, 5% Tween 80, and 90% saline (0.9% NaCl). Docetaxel was provided by Sanofi-Aventis as a white powder and was dissolved in ethanol/polysorbate 80 as a stock solution and diluted 10-fold in 5% glucose for *in vivo* studies.

Binding Studies

Tubulin assays with SG410 and SG430 were done as previously described (20, 21). Briefly, tubulin polymerization was followed turbidimetrically at 350 nm in Beckman model DU7400 and DU7500 recording spectrophotometers equipped with electronic temperature controllers. Reaction mixtures contained 1.0 mg/mL tubulin (10 μmol/L), 0.8 mol/L monosodium glutamate, 4% DMSO, and varying drug concentrations. Samples were pre-incubated for 15 min at 30°C and chilled on ice. GTP (final concentration, 0.4 mmol/L) was added to each reaction mixture, and these were placed in cuvettes held at 0°C. Baselines were established, the temperature was raised to 30°C (~0.5°C/s for 30 s), and polymerization was followed for 20 min. IC_{50} values were determined by graphical interpolation of experimental points, with drug-containing samples compared with control reaction mixtures containing DMSO but no drug. At least three independent IC_{50} values were obtained with each compound. Combretastatin A-4 was generously provided by Dr. George R. Pettit (Arizona State University, Tempe, AZ).

Cell Lines and *In vitro* Culture Conditions

The cell lines ASPC1, MiaPaca2, HS766T, and L36PL were obtained from the American Tissue Culture Collection and are derived from pancreas carcinomas. The cell lines Panc1, Panc203, and Panc1005 are low-passage pancreas cell lines and were a kind gift from Dr. Elizabeth Jaffee (Johns Hopkins University School of Medicine, Baltimore, MD). The cell lines XPA3 and XPA4 are low-passage pancreas cell lines and were a kind gift from Dr. Anirban Maitra (Johns Hopkins University School of Medicine). The cell lines E3LZ10 and E3JD13 are low-passage pancreas cell lines obtained from a rapid autopsy program and were a kind gift from Dr. Christine Iacobuzio-Donahue (Johns Hopkins University School of Medicine). For clonogenic assessment, 500 cells per well were seeded in six-well plates with enriched RPMI (10% fetal bovine serum + 1% penicillin/streptomycin) and exposed to increasing drug concentrations for 96 h. After this, the drug was removed, and the cells were allowed to grow for 14 days before manual colony counting. Each experiment was done in duplicate for each drug concentration and was carried out independently at least thrice. For MAPT protein and mRNA expression analysis, the cell lines were grown in six-well plates with enriched RPMI. When the cells reached a 60% to 70% confluence, they were washed twice with chilled PBS; lysis buffer was added to the plates; and the cells were scraped for protein extraction. An identical experimental set was lysed with RLT (Qiagen) for mRNA extraction.

In vivo Growth Inhibition Studies

Six-week-old female athymic nude mice (Harlan) were used. The research protocol was approved by the Johns Hopkins University Animal Care and Use Committee, and animals were maintained in accordance to guidelines of the American Association of Laboratory Animal Care. Surgical non-diagnostic specimens from patients who had undergone surgery at the Johns Hopkins Hospital were implanted s.c. in one to two mice for each patient, with two small pieces per mouse (F1 generation). Tumors were grown to 1.5 cm^3 and then harvested, divided into small ~3 × 3 × 3 mm pieces, and transplanted to another five mice, with two tumors per mouse (F2 generation). After a second growth passage, tumors were excised and propagated to cohorts of ≥20 mice. These groups constituted the F3, or treatment cohort. Tumors from this third mouse-to-mouse passage were allowed to grow to ~200 mm^3, at which time mice were randomized into three treatment groups, with five to six mice (10 evaluable

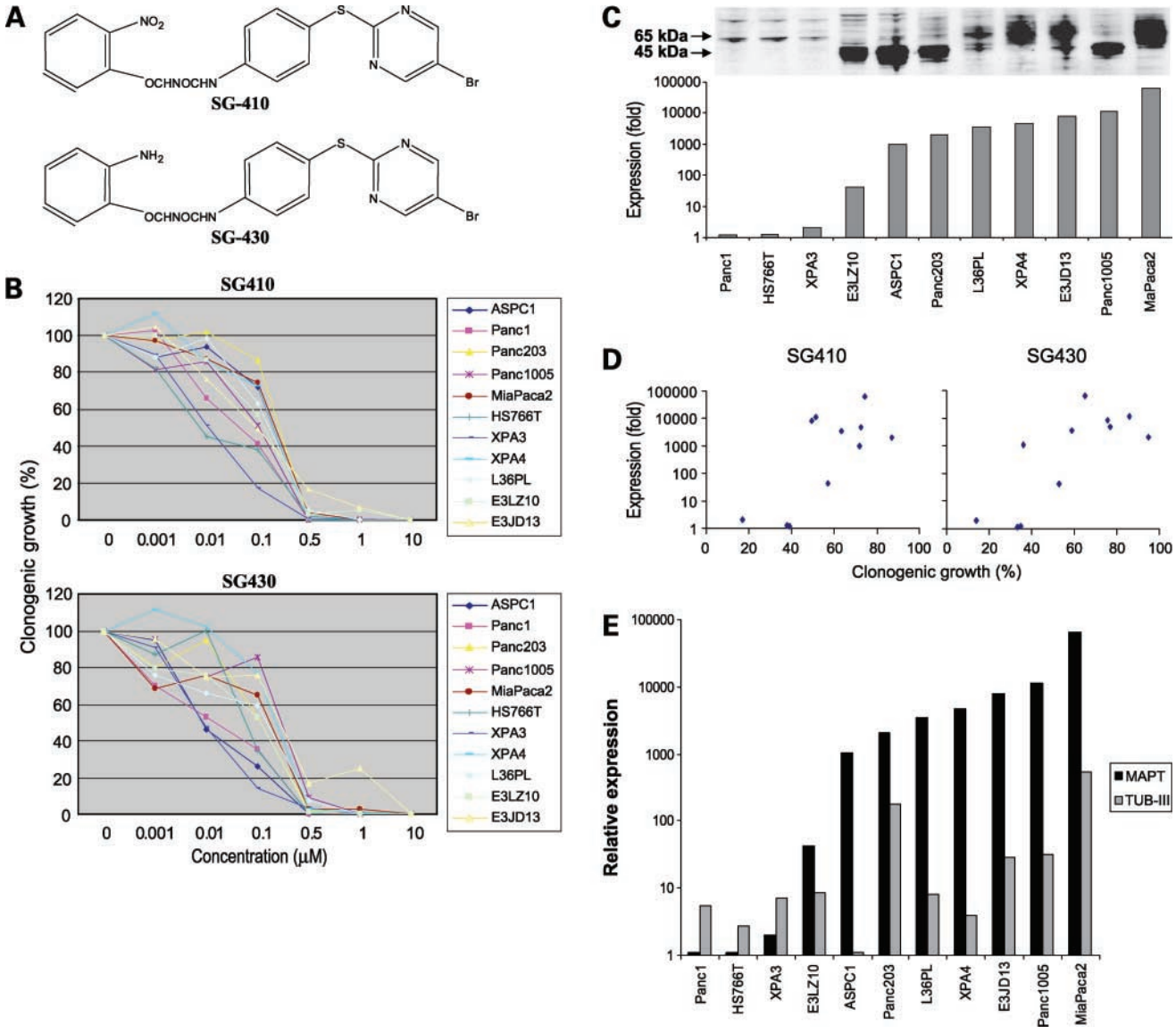

Figure 1. **A,** chemical structure of SG410 and SG430. **B,** clonogenic growth after exposure to each of the drugs for 96 h. Two cell lines had their clonogenic capability significantly impaired by SG410 in the 1 to 10 nmol/L range (HS766T and XPA3) and three cell lines (Panc1, XPA3, and ASPC1) by SG430. With both drugs, the most resistant cell line was E3JD13, with which there was a low level of colony viability at concentrations of $\geq$1 μmol/L. **C,** MAPT mRNA levels varied across a wide range (65,000-fold). There was a significant correlation between mRNA and protein, with the three lowest mRNA-expressing cells lines also showing low protein expression. Two isoforms of MAPT protein were detected (45 and 65 kDa), with a distinct distribution. The cell lines with lowest mRNA expression showed traces of the 65-kDa isoform, whereas there was a degree of polarity in the other except L36PL that expressed both. In the high protein-expressing cell lines, no correlation between isoform expression and activity was detected. **D,** correlation between clonogenic growth (*X*-axis) at 0.1 μmol/L and MAPT mRNA levels (*Y*-axis) in the panel of cell lines. **E,** comparison of the expression of class III β-tubulin and MAPT in the panel of cell lines.

tumors) in each group: control (vehicle), G410 (50 mg/kg i.p. twice per week), and G430 (50 mg/kg i.p. twice per week). Docetaxel treatment was given to selected groups at a dose of 30 mg/kg i.p. once a week for 2 weeks. Mice were monitored daily for signs of toxicity and were weighed thrice per week. Tumor size was evaluated twice per week by caliper measurements using the following formula: tumor volume = [length $\times$ width^2] / 2. Relative tumor growth inhibition was calculated by relative tumor growth of treated mice divided by relative tumor growth of control mice from the onset of therapy (T/C).

Quantitative Real-time Reverse Transcription-PCR Analysis

Total RNA was extracted from cell pellets and tumors using the RNeasy Mini kit (Qiagen). cDNA was synthesized using the iScript cDNA synthesis kit (Bio-Rad), following the manufacturer's instructions. Relative quantification of MAPT, class III β-tubulin, and housekeeper

ubiquitin C mRNA was achieved using an iCycler iQ real-time PCR detection system (Bio-Rad) using ABI Taqman probes. Accumulation of the specific PCR products was detected as an increase in fluorescence that was plotted against cycle number to determine the CT values. Relative expression of the mRNA analyzed was estimated using the formula: $2^{-\Delta CT}$, where $\Delta C_T = C_T$ (mRNA) $- C_T$ (ubiquitin C). Samples were analyzed in a blinded manner.

Western Blot Analysis

Equal amounts of protein were resolved on 10% polyacrylamide gels. Gels were transferred onto nitrocellulose membranes that were incubated overnight at 4°C with antibodies against MAPT and actin (Santa Cruz Biotechnology). The immunoreactive proteins were detected using the enhanced chemiluminescence method (Amersham).

DNA Sequencing Analysis

DNA was extracted from the cell line pellets and frozen tumors, tested by means of selection with specific primers, amplification with PCR, and sequencing of the different exons and introns that constitute the gene and are known to harbor mutations (*MAPT*: exons 9–13) or the complete gene (*TUBB*: exons 1–4). The following primers were designed/used to sequence the *MAPT* gene: exon 9, forward 5′-CTGCCTAACCCAGTGGTGA-3′ and reverse 5′-CACAGTCCCACGACTCCAC-3′; exon 10, forward 5′-CTCTGCCAAGTCCGAAAGTG-3′ and reverse 5′-ATCCTGAGAGCCCAAGAAGG-3′; exon 11, forward 5′-ATAAGGGCCTGGGCTTACAC-3′ and reverse 5′-CCGCAAGTTTCACACTCAAC-3′; exon 12, forward 5′-TTCAAGTCCTGCTGCAAACC-3′ and reverse 3′-CTCCAGGTGATTGAGACAGG-3′; exon 13, forward 5′-AGGCTGCAGTGAGGTGAGAT-3′ and reverse 5′-CCGAGTGACAAAAGCAGGTT-3′ (Invitrogen/Life Technologies). The following primers were designed/used to sequence the *TUBB* gene: exon 1, forward 5′-TACATGACCGGCATCGACTA-3′ and reverse 5′-ACAAACTTGAGAGGGGCAAA-3′; exons 2 and 3, forward 5′-AGCGAGACTCCGTCTCAAAA-3′ and reverse 5′-CTTTTGCTGTGTCCTTGCAC-3′; exon 4a, forward 5′-CGAGGGAATTATTTGAAAAGTTG-3′ and reverse 5′-GGCATCGAAGACCTGCTG-3′; exon 4b, forward 5′-TTCTTTATGCCTGGCTTTGC-3′ and reverse 3′-CCCAGAATGGCAGAAACCTA-3′; exon 4c, forward 5′-TCCCTCAGAATTTGTGTTTGC-3′ and reverse 5′-GCTCGAGTGAGGGAGGTAGA-3′; exon 4d, forward 5′-TGTCAGCAGTATTATCTCCACTTT-3′ and reverse 5′-TTAAGTGTCAATTTAAGGAGA-3′ (Invitrogen/Life Technologies). The 25-μL PCR reaction consisted of 0.2 μmol/L concentration of each outside primer along with 150 ng of genomic DNA, HotMaster Mix 2.5× (Eppendorf) containing 960 μmol/L deoxynucleotide triphosphates, 54 mmol/L KCl, 3.0 mmol/L $MgCl_2$, and 0.6 units of Taq Polymerase. Thermocycler conditions were initial cycle at 95°C for 3 min, followed by 10 cycles 94°C for 45 s, 57.6°C for 1 min, and 72°C for 1 min; 20 cycles of 89°C for 1 min, 57.6°C for 1 min, and 72°C for 1 min. PCR product clean-up consisted of 3 μL Shrimp Alkaline Phosphatase and 0.3 μL Exonuclease1 (GE Healthcare) per sample incubated at 37°C for 1 h followed by one step of 80°C for 15 min. The existence of a variant was determined by direct nucleotide sequencing. Sequencing was done using an ABI 3730XL Sequencer (Applied Biosystems), following standard dideoxy terminator protocols (22, 23). Sequences were analyzed using Sequencher (Genecodes). Only changes present in both strands were identified as single nucleotide polymorphisms.

Statistical Analysis

To assess the treatment effect, a hierarchical linear regression model was used with random intercepts and fixed slopes. Based on the results of exploratory plots, the assumption of fixed effects for slopes seemed reasonable. This model allowed for mouse effects to be nested within patient effects so that the hierarchical structure is fully accounted for. Specifically, we fit the following linear regression model:

$$\log(y_{ijt}) = a_{1ij}\text{time}_{ijt} + b_{2j}\text{time}_{ijt} \times trt_{ij} + \beta\text{time}_{ijt}^2 + e_{ijt}$$

where j indexes patient, i indexes mouse, and t indexes time; y_{ijt} is the percentage change in tumor volume (compared with day 0) in mouse i, which is a xenograft for patient j at time t; and trt_{ij} is treatment (1 = treated, 0 = control) received by mouse i, which is a xenograft for patient j. We explored a series of models to determine a good fitting model and found that the above model was adequate. An intercept and main effect of treatment were not included in the model that makes two assumptions: (*a*) at time 0, the change from baseline is 0 (which is empirically true), and (*b*) at baseline, the treated and untreated curves intersect. The model was fit using WinBugs software that estimates models using a Markov chain Monte Carlo estimation procedure. A burn-in of 10,000 iterations was done, and then the chain was run for an additional 20,000 iterations, of which every 10th iteration was saved for inference. Several chains were run with different starting values to ensure convergence. No convergence issues arose. The fitted model was used to make inferences with respect to the treatment effect and to create fitted regression lines (rescaled on the Y-axis for clearer interpretation). Point estimates of variables of interest (e.g., expected difference in tumor volume between treated and control at 28 days) and 95% credible intervals were based on the mean of posterior distributions and the 2.5th and 97.5th quantiles of the posterior distribution, respectively. The comparisons between means and proportions obtained from the biological studies were done using Student's t test and χ^2 method, respectively. ANOVA was used when three or more variables were compared.

Results

Binding Properties

Because benzoylphenylurea derivatives were first identified as anti-mitotic agents that inhibited tubulin assembly and inhibited colchicine binding to tubulin (24), we

examined SG410 and SG430 for similar effects with purified tubulin in comparison with combretastatin A-4, one of the most potent inhibitors of colchicine binding yet discovered (21). As shown in Table 1, SG410 was more active than SG430 in both assays. In the polymerization study, SG410 was slightly more active than combretastatin A-4 (IC_{50}, 1.2 and 1.4 μmol/L, respectively), whereas SG430 was half as active (IC_{50}, 3.0 μmol/L). In the colchicine-binding assay, both of the benzoylphenylureas were substantially less active than combretastatin A-4 probably because these compounds dissociate rapidly from the colchicine site. Colchicine, in contrast, binds slowly to tubulin and, once bound, dissociates extremely slowly ($t_{1/2} \geq 24$ h, depending on reaction conditions).

In vitro Growth Inhibition Analysis and Correlation between Putative Markers and Efficacy

Both drugs showed similar effects on the 11 pancreatic cancer cell line panel. Clonogenic growth was impaired at concentrations between 0.01 and 0.5 μmol/L (Fig. 1B), with no colony formation at higher doses in 9 of the 11 cell lines. MAPT mRNA levels varied over a wide (65,000-fold) range (Fig. 1C). Expression was normalized to the lowest sample, which was arbitrarily assigned a value of 1. There was a correlation between mRNA and protein, with the three lowest mRNA-expressing cells lines showing a low protein expression. Two isoforms of MAPT protein were detected (45 and 65 kDa). The three cell lines with lower MAPT mRNA levels expressed traces of the 65-kDa isoform. The 45-kDa isoform predominates in E3LZ10, ASPC1, Panc203, and Panc1005 (the second highest MAPT-expressing cell line), whereas the 65-kDa isoform predominates in XPA4, E3JD13, and MiaPaCa2 (the highest MAPT-expressing cell line). The two MAPT isoforms seemed equally expressed in L36PL.

At the most discriminative concentrations of both drugs (0.01 and 0.1 μmol/L), the three most sensitive cell lines were consistently those with lower MAPT levels (Panc1, HS766T, and XPA3) and showed a 10-fold superior sensitivity than those with higher levels of MAPT. In the eight high protein-expressing cell lines, no correlation between isoform expression and activity was detected. In Fig. 1D, the clonogenic growth at 0.1 μmol/L for both drugs and the MAPT mRNA levels of the cell lines is depicted. Treatment did not induce variations in MAPT mRNA levels.

Table 1. Inhibition of tubulin polymerization and colchicine binding by compounds SG410 and SG430

Compound	Tubulin*, IC_{50} ± SD (μmol/L)	Colchicine binding† (% ± SD)
SG410	1.2 ± 0.1	29 ± 4
SG430	3.0 ± 0.3	20 ± 5
Combretastatin A-4	1.4 ± 0.1	100 ± 0.7

*Inhibition of tubulin polymerization: tubulin was at 10 μmol/L (20).
†Inhibition of [^{3}H]colchicine binding: tubulin was at 1 μmol/L; both [^{3}H]colchicine and inhibitor were at 5 μmol/L (21).

In vivo Dose-Finding Study

Both drugs were explored by the i.p. route in cohorts of six mice each, with a duration of treatment of 4 weeks. The two initial dose levels of both compounds (20 mg/kg twice per week and 30 mg/kg twice per week) were not associated with noticeable toxicity. Therefore, 50 mg/kg twice per week was explored. One of six mice in the SG410 group had a weight loss of 15% by the 4th week, but no deaths occurred. Therefore, the dose was escalated to 50 mg/kg thrice per week. In the SG410 and SG430 groups, respectively, two and one of the mice died in the 3rd week, and three of four and four of five of the remaining animals lost >15% of their weight. Thus, for 28-day efficacy studies following an i.p. route, we selected 50 mg/kg twice a week for both compounds.

In vivo Growth Inhibition Analysis

Tumors from nine cases of pancreatic cancer were used to establish xenografts in nude mice, and the animals were treated with either vehicle, SG410, or SG430 (Fig. 2A). The level of efficacy varied both between drugs and within cases treated with each drug. Figure 3 provides an integrated summary of all data points obtained in the studies. Overall, there were no statistical differences between the slopes of the treated versus control group for either of the agents, although SG410 showed a greater efficacy than SG430. Assessment of individual groups, as shown in Fig. 2A, shows that in SG410-treated tumors, four cases had an average growth after 28 days of treatment of ≤50%, and a fifth had 60%. In contrast, SG430 induced significant growth arrest in only two cases with growths of 43% and 59%.

In vivo Correlation between MAPTand Efficacy

To gain insight into factors that could at least partially explain the observed observations, we determined the expression of MAPT in the patient tumor xenografts. Expression was normalized to the lowest sample, which was arbitrarily assigned a value of 1. There was a correlation between mRNA and protein, with the three highest mRNA-expressing cases showing significant protein expression by Western blot. The five cases with the lowest MAPT expression were those where SG410 showed a tumor growth reduction that was statistically significant compared with their respective control groups; or, inversely, in all cases with low MAPT levels, SG410 was able to significantly inhibit tumor growth. However, one of those, despite being significant, was not considered relevant, as the T/C was 60%. The comparison of the proportion of sensitive cases according to having below (4 of 5) or above (0 of 4) the median MAPT expression is statistically significant (two-sided Fisher's test, $P = 0.048$). SG430 induced growth arrest in two cases with minimal expression of MAPT, but this trend is weaker than with SG410, as fewer cases were sensitive. Consequently, the predictive value for SG430 is lower.

Comparison of SG410 and SG430 *In vivo* Activity with Docetaxel

Three of the cases were also treated with docetaxel to compare the efficacy of the benzoylphenylurea agents with

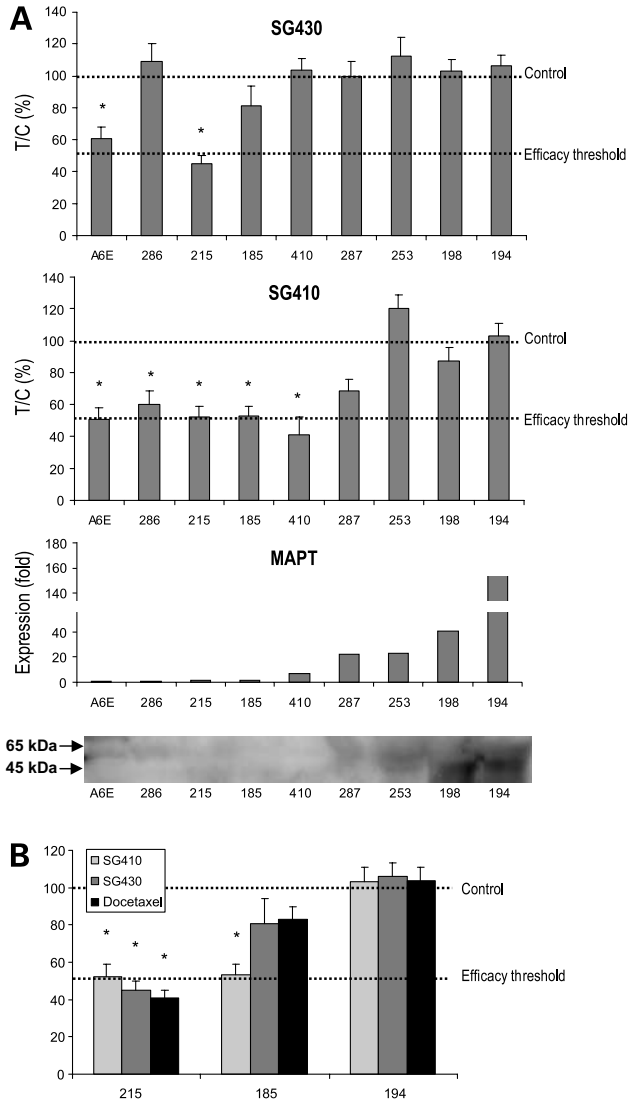

Figure 2. *In vivo* growth of pancreas cancer xenografts treated with the study drugs. The growth of the control group from the day treatment started to day 28 of the experiment was set as the reference (100%). *Columns,* growth (%) normalized to the untreated group for each case; *bars,* SE. **A,** SG430 inhibited growth of two cases (215 and A6E), but the latter corresponded to a modest 59% growth relative to control. SG410 showed a greater efficacy, particularly in the five cases with lower MAPT expression. **B,** SG410 and SG430 compared with docetaxel treatment. The level of efficacy in 215 was comparable between the three treatment groups (ANOVA, $P = 0.47$). However, SG410 was more active than SG430 and docetaxel in another low MAPT case (185; ANOVA, $P = 0.05$). Neither of the three treatments induced any significant tumor growth arrest in 194, a case with 160-fold higher MAPT expression than 215. *Columns,* efficacy ($n = 10$ tumors per group); *bars,* SE. *, $P < 0.05$, compared with control (Student's *t* test).

an established anticancer agent targeting microtubules and also to determine the correlation of such efficacy and MAPT expression (Fig. 2B). Docetaxel, as was the case with both SG410 and SG430, was particularly efficacious in 215, a low MAPT-expressing case. Docetaxel showed lower efficacy than SG410 in 185, and all three compounds were inactive in 194, a case with the greatest expression of MAPT among those examined.

Analysis of Class III β-Tubulin Expression and MAPT and Class I β-Tubulin Mutations

The level of expression of class III β-tubulin was also assessed in the cell lines and in the tumors. Although among the lowest expressing cell lines for class III β-tubulin were HS766T and Panc1, and the highest was MiaPaCa2, the correlation for the group of cell lines as a whole was poor (Fig. 1E), and there was not a correlation between class III β-tubulin and efficacy. In addition, there was neither a correlation between MAPT and class III β-tubulin in the xenografts nor a relationship with efficacy (the highest expression of class III β-tubulin corresponded to A6E and 286, and resistant cases had low or intermediate expression such as 194 or 253; data not shown). No mutations or polymorphisms in exons 9, 10, 11, 12, and 13 of MAPT or in exons 1, 2, 3, and 4 of class I β tubulin were found in the tested panel of cell lines ($n = 11$) and patient xenograft cases used in the *in vivo* studies ($n = 9$).

Discussion

In this work, we evaluated the two leading compounds obtained from a screen of sulfur benzoylphenylurea analogues (11) against *in vitro* and *in vivo* models of pancreas cancer. We determined the best administration schedule and tested both SG410 and SG430 in a novel platform of direct pancreas cancer xenografts taken from patient tumors. Our studies showed that SG410 is the best candidate for further development. In addition, we found that MAPT expression in pancreas tumor cells and tissue is a marker that thus far predicts the efficacy of SG410.

In our studies aimed at developing these benzoylphenylurea analogues as drugs and in showing that MAPT should be a valuable predictive biomarker, we used as a model pancreas cancer xenografts grown from tumors removed from human patients (12). Generally, before entering clinical trials, new agents are tested against high-passage cell lines and xenografts established from these lines. It is unclear how representative those models are of the biology of pancreas cancer. Although the predictive utility of our patient-derived xenograft model is currently being evaluated in a prospective, controlled clinical trial, it has several features that are intuitively appealing. It has been shown to be feasible, with a high engraftment rate. Even more importantly for new drug development, the patient-derived xenografts are stable over time and passages, both genetically and from the perspective of drug sensitivity. The ability to test several drugs simultaneously allows for direct comparisons, and the availability of large amounts of tissue permits the performance of detailed biological analyses as well as the development of novel techniques for seriated pharmacodynamic assessment. As opposed to cell line–derived *in vivo* models, in these xenografts (as in the clinic), regressions occur infrequently. Therefore, growth retardation is the primary end point used to determine the efficacy of tested agents.

Both SG410 and SG430 had antiproliferative activity *in vitro* in the low nanomolar range and showed a similar mechanism of action, with the former twice as potent as the latter as an inhibitor of tubulin assembly. This probably accounts for the greater *in vivo* activity of SG410. This is consistent with the finding that increased levels of MAPT were associated with resistance to these benzoylphenylurea analogues because MAP, including MAPT, strongly enhance tubulin assembly. However, there were differences for which we do not have an explanation, such as the sensitivity to SG410 and resistance to SG430 of 286, a case with low MAPT. Other factors are likely to intervene. Another finding was that in a limited direct comparison in three of the cases, SG410 was at least as efficacious (if not better) than docetaxel, an active anticancer agent with some activity in pancreas cancer (25). It is difficult to interpret the relevance of this observation, as docetaxel has not been systematically studied in this disease. In comparison with other agents tested in the same patient-derived xenografts, SG410 was superior to erlotinib but less active than gemcitabine (12).

Limited information regarding factors relevant to the efficacy of a drug at initiation of clinical trials may be responsible for the low yield rate in anticancer drug development, including pancreatic cancer. Given the complexities of cancer, a given agent is usually only active in a fraction of patients with a specific tumor type. Therefore, identifying the factors leading to a positive response to treatment will not only help prevent unnecessary therapy but also, if discovered in early stages of drug development, may prove instrumental in the ultimate success of the drug (26).

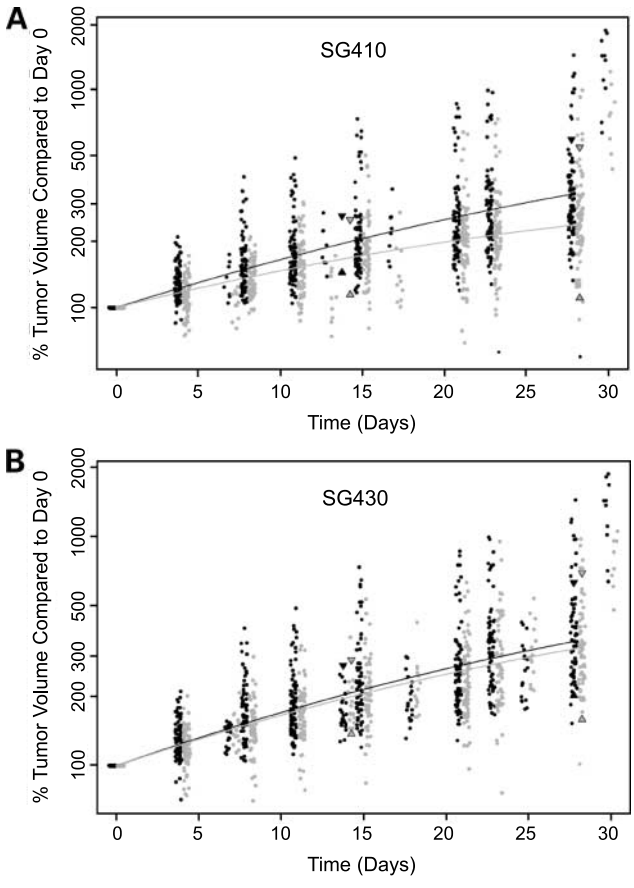

Figure 3. Integrated analysis of all the data points from the nine treatment groups for SG410 (**A**) and SG430 (**B**). *Black dots,* control tumors; *gray dots,* treated tumors.

Here, we explored the potential value of MAPT, a protein that binds to microtubules and enhances their assembly and stability and that has been linked to sensitivity to paclitaxel and docetaxel (16, 17). In both the cell lines and the patient-derived xenografts, there was an exquisite correlation between mRNA and protein levels, which increases the likelihood of developing a feasible diagnostic test for clinical use. Equally important, there was also a solid, inverse correlation between MAPT expression and sensitivity to all tested agents. Specifically, the same inverse correlation between MAPT and SG410/SG430 activity occurred with docetaxel (both in prior clinical data and in the preclinical experiments presented here), despite the opposing mechanisms of action of benzoylphenylureas and taxanes (inhibition of tubulin assembly versus enhancement of assembly, respectively). As was noted above, the inverse correlation of MAPT expression with drug sensitivity is readily understood with the benzoylphenylurea analogues because MAP in general strongly enhance microtubule formation and thus may reduce the effect of drugs that interfere with microtubule formation.

In 1994, an autosomal dominantly inherited form of frontotemporal dementia with parkinsonism was linked to chromosome 17q21.2 (27), an association that was subsequently found in other patients, leading to designation of frontotemporal dementia and parkinsonism linked to chromosome 17Q (FTDP-17) as diagnostic category. In all cases of FTDP-17, a filamentous pathologic body made of MAPT protein is found, and in 1998, the first mutations in the *MAPT* gene in FTDP-17 patients were reported (28–30). Currently, 32 different mutations have been described in over 100 families with FTDP-17. MAPT mutations are either missense mutations, deletions, or silent mutations in the coding region. MAPT mutations fall into two largely non-overlapping categories: those that influence the alternative splicing of MAPT pre-mRNA and those whose primary effect is at the protein level. Several mutations in exon 10 of MAPT, such as DK280, DN296, and N296H, have effects at both mRNA and protein levels (31–33). We speculated that the differences in mRNA and protein expression of MAPT in the pancreas cancer cell lines and xenografts could have been related to presence of mutations or polymorphisms, but none were found after sequencing the five exons most frequently affected by these genetic variants. In addition, no mutations were found in the class I *β-tubulin* gene. Despite the initial report of such mutations being related to taxane sensitivity in lung cancer, subsequent reports have suggested that their frequency may be lower (34, 35).

There are limitations to the work presented here. First, although highly active *in vitro*, SG410 *in vivo* activity was significant in five of nine tested cases, albeit relatively modest, and no regressions were observed. Second, this family of compounds shows poor aqueous solubility, resulting in unpredictable pharmacokinetics (9). A major goal for the future is the development of an active, soluble analogue. This should lead to an orally available formulation, enhanced exposure of tumor to drug, and more predictable pharmacologic properties.

In summary, a rational stepwise screening of sulfur benzoylphenylurea derivatives in models of pancreas cancer has identified SG410 as an agent with potential for further development in pancreas cancer. It has shown at least comparable efficacy with docetaxel in direct comparisons and superior historical activity to other agents approved for pancreatic cancer, such as erlotinib, based on our previous data. Additionally, we have found evidence suggesting that MAPT levels may help in identifying patients more likely to benefit from the drug, which would represent a step forward in the individualization of cancer therapy.

References

1. Jemal A, Siegel R, Ward E, et al. Cancer statistics, 2006. CA Cancer J Clin 2006;56:106 – 30.

2. Yeo TP, Hruban RH, Leach SD, et al. Pancreatic cancer. Curr Probl Cancer 2002;26:176 – 275.

3. Downing KH, Nogales E. Tubulin structure: insights into microtubule properties and functions. Curr Opin Struct Biol 1998;8:785 – 91.

4. Sorger PK, Dobles M, Tournebize R, Hyman AA. Coupling cell division and cell death to microtubule dynamics. Curr Opin Cell Biol 1997;9: 807 – 14.

5. Jordan A, Hadfield JA, Lawrence NJ, McGown AT. Tubulin as a target for anticancer drugs: agents which interact with the mitotic spindle. Med Res Rev 1998;18:259 – 96.

6. Okada H, Koyanagi T, Yamada N, Haga T. Synthesis and antitumor activities of novel benzoylphenylurea derivatives. Chem Pharm Bull (Tokyo) 1991;39:2308 – 15.

7. Okada H, Koyanagi T, Yamada N. Synthesis and antitumor activities of prodrugs of benzoylphenylureas. Chem Pharm Bull (Tokyo) 1994;42: 57 – 61.

8. Okada H, Kato M, Koyanagi T, Mizuno K. Synthesis and antitumor activities of water-soluble benzoylphenylureas. Chem Pharm Bull (Tokyo) 1999;47:430 – 3.

9. Rudek MA, Zhao M, Smith NF, et al. *In vitro* and *in vivo* clinical pharmacology of dimethyl benzoylphenylurea, a novel oral tubulin-interactive agent. Clin Cancer Res 2005;11:8503 – 11.

9a. Messersmith WA, Rudek MA, Baker SD, et al. Phase I study of continuous weekly dosing of dimethylamino benzoylphenylurea (BPU) in patients with solid tumors. Eur J Cancer 2007;43:78 – 86.

10. Gurulingappa H, Amador ML, Zhao M, et al. Synthesis and antitumor evaluation of benzoylphenylurea analogs. Bioorg Med Chem Lett 2004;14: 2213 – 6.

11. Hallur G, Jimeno A, Dalrymple S, et al. Benzoylphenylurea sulfur analogues with potent antitumor activity. J Med Chem 2006;49: 2357 – 60.

12. Rubio-Viqueira B, Jimeno A, Cusatis G, et al. An *in vivo* platform for translational drug development in pancreatic cancer. Clin Cancer Res 2006;12:4652 – 61.

13. Goedert M, Wischik CM, Crowther RA, Walker JE, Klug A. Cloning and sequencing of the cDNA encoding a core protein of the paired helical filament of Alzheimer disease: identification as the microtubule-associated protein tau. Proc Natl Acad Sci U S A 1988;85:4051 – 5.

14. Goedert M, Spillantini MG, Potier MC, Ulrich J, Crowther RA. Cloning and sequencing of the cDNA encoding an isoform of microtubule-associated protein tau containing four tandem repeats: differential expression of tau protein mRNAs in human brain. EMBO J 1989;8:393 – 9.

15. Goedert M, Spillantini MG, Jakes R, Rutherford D, Crowther RA. Multiple isoforms of human microtubule-associated protein tau: sequences and localization in neurofibrillary tangles of Alzheimer's disease. Neuron 1989;3:519 – 26.

16. Veitia R, Bissery MC, Martinez C, Fellous A. Tau expression in model adenocarcinomas correlates with docetaxel sensitivity in tumour-bearing mice. Br J Cancer 1998;78:871 – 7.

17. Rouzier R, Rajan R, Wagner P, et al. Microtubule-associated protein tau: a marker of paclitaxel sensitivity in breast cancer. Proc Natl Acad Sci U S A 2005;102:8315 – 20.

18. Seve P, Mackey J, Isaac S, et al. Class III beta-tubulin expression in tumor cells predicts response and outcome in patients with non-small cell lung cancer receiving paclitaxel. Mol Cancer Ther 2005;4:2001 – 7.

19. Monzo M, Rosell R, Sanchez JJ, et al. Paclitaxel resistance in non-small-cell lung cancer associated with beta-tubulin gene mutations. J Clin Oncol 1999;17:1786 – 93.

20. Hamel E. Evaluation of antimitotic agents by quantitative comparisons of their effects on the polymerization of purified tubulin. Cell Biochem Biophys 2003;38:1 – 22.

21. Verdier-Pinard P, Lai JY, Yoo HD, et al. Structure-activity analysis of the interaction of curacin A, the potent colchicine site antimitotic agent, with tubulin and effects of analogs on the growth of MCF-7 breast cancer cells. Mol Pharmacol 1998;53:62 – 76.

22. Smith LM, Sanders JZ, Kaiser RJ, et al. Fluorescence detection in automated DNA sequence analysis. Nature 1986;321:674 – 9.

23. McCombie WR, Heiner C, Kelley JM, Fitzgerald MG, Gocayne JD. Rapid and reliable fluorescent cycle sequencing of double-stranded templates. DNA Seq 1992;2:289 – 96.

24. Paull KD, Lin CM, Malspeis L, Hamel E. Identification of novel antimitotic agents acting at the tubulin level by computer-assisted evaluation of differential cytotoxicity data. Cancer Res 1992;52:3892 – 900.

25. Rougier P, Adenis A, Ducreux M, et al. A phase II study: docetaxel as first-line chemotherapy for advanced pancreatic adenocarcinoma. Eur J Cancer 2000;36:1016 – 25.

26. Slamon DJ, Leyland-Jones B, Shak S, et al. Use of chemotherapy plus a monoclonal antibody against HER2 for metastatic breast cancer that overexpresses HER2. N Engl J Med 2001;344:783 – 92.

27. Wilhelmsen KC, Lynch T, Pavlou E, Higgins M, Nygaard TG. Localization of disinhibition-dementia-parkinsonism-amyotrophy complex to 17q21-22. Am J Hum Genet 1994;55:1159 – 65.

28. Poorkaj P, Sharma V, Anderson L, et al. Missense mutations in the chromosome 14 familial Alzheimer's disease presenilin 1 gene. Hum Mutat 1998;11:216 – 21.

29. Hutton M, Lendon CL, Rizzu P, et al. Association of missense and 5′-splice-site mutations in tau with the inherited dementia FTDP-17. Nature 1998;393:702 – 5.

30. Spillantini MG, Murrell JR, Goedert M, et al. Mutation in the tau gene in familial multiple system tauopathy with presenile dementia. Proc Natl Acad Sci U S A 1998;95:7737 – 41.

31. D'Souza I, Poorkaj P, Hong M, et al. Missense and silent tau gene mutations cause frontotemporal dementia with parkinsonism-chromosome 17 type, by affecting multiple alternative RNA splicing regulatory elements. Proc Natl Acad Sci U S A 1999;96:5598 – 603.

32. Rizzu P, Van Swieten JC, Joosse M, et al. High prevalence of mutations in the microtubule-associated protein tau in a population study of frontotemporal dementia in the Netherlands. Am J Hum Genet 1999; 64:414 – 21.

33. Yoshida H, Crowther RA, Goedert M. Functional effects of tau gene mutations deltaN296 and N296H. J Neurochem 2002;80:548 – 51.

34. Sale S, Sung R, Shen P, et al. Conservation of the class I beta-tubulin gene in human populations and lack of mutations in lung cancers and paclitaxel-resistant ovarian cancers. Mol Cancer Ther 2002;1: 215 – 25.

35. Achiwa H, Sato S, Shimizu S, et al. Analysis of beta-tubulin gene alteration in human lung cancer cell lines. Cancer Lett 2003;201:211 – 6.